Effects of Hydrogen Bonding to a Bacteriochlorophyll−Bacteriopheophytin Dimer in Reaction Centers from *Rhodobacter sphaeroides*†

J. P. Allen,* K. Artz, X. Lin, and J. C. Williams

Department of Chemistry and Biochemistry and Center for the Study of Early Events in Photosynthesis, Arizona State University, Tempe, Arizona 85287-1604

A. Ivancich, D. Albouy, and T. A. Mattioli

Section de Biophysique des Protéines et des Membranes, Département de Biologie Cellulaire et Moléculaire, CEA and URA CNRS 1290, C. E. de Saclay, 91191 Gif-sur-Yvette Cedex, France

A. Fetsch, M. Kuhn, and W. Lubitz

Max-Volmer-Institut für Biophysikalische Chemie und Biochemie, Technische Universität Berlin, Strasse des 17 Juni 135, D-10623 Berlin, Germany

Received November 29, 1995; Revised Manuscript Received March 7, 1996⊗

ABSTRACT: The properties of the primary electron donor in reaction centers from *Rhodobacter sphaeroides* have been investigated in mutants containing a bacteriochlorophyll (BChl)−bacteriopheophytin (BPhe) dimer with and without hydrogen bonds to the conjugated carbonyl groups. The heterodimer mutation His M202 to Leu was combined with each of the following mutations: His L168 to Phe, which should remove an existing hydrogen bond to the BChl molecule; Leu L131 to His, which should add a hydrogen bond to the BChl molecule; and Leu M160 to His and Phe M197 to His, each of which should add a hydrogen bond to the BPhe molecule [Rautter, J., Lendzian, F., Schulz, C., Fetsch, A., Kuhn, M., Lin, X., Williams, J. C., Allen, J. P., & Lubitz, W. (1995) *Biochemistry 34*, 8130−8143]. Pigment extractions and Fourier transform Raman spectra confirm that all of the mutants contain a heterodimer. The bands in the resonance Raman spectra arising from the BPhe molecule, which is selectively enhanced, exhibit the shifts expected for the addition of a hydrogen bond to the 9-keto and 2-acetyl carbonyl groups. The oxidation−reduction midpoint potential of the donor is increased by approximately 85 mV by the addition of a hydrogen bond to the BChl molecule but is only increased by approximately 15 mV by the addition of a hydrogen bond to the BPhe molecule. An increase in the rate of charge recombination from the primary quinone is correlated with an increase in the midpoint potential. The yield of electron transfer to the primary quinone is 5-fold reduced for the mutants with a hydrogen bond to the BPhe molecule. Room- and low-temperature optical absorption spectra show small differences from the features that are typical for the heterodimer, except that a large increase in absorption is observed around 860−900 nm for the donor Q_y band in the mutant that adds a hydrogen bond to the BChl molecule. The changes in the optical spectra and the yield of electron transfer are consistent with a model in which the addition of a hydrogen bond to the BChl molecule increases the energy of an internal charge transfer state while the addition to the BPhe molecule stabilizes this state. The results show that the properties of the heterodimer are different depending on which side is hydrogen-bonded and suggest that the hydrogen bonds alter the energy of the internal charge transfer state in a well-defined manner.

The site of the primary photochemistry in photosynthesis is an integral membrane pigment−protein complex termed the reaction center [for reviews see Parson (1991), Kirmaier and Holten (1993), and Woodbury and Allen (1995)]. Light causes the excitation of the primary donor P,[1] which transfers an electron to a series of acceptors. The three-dimensional structure of the reaction center from *Rhodobacter sphaeroides* has been determined by X-ray diffraction (Allen et al., 1987; El-Kabbani et al., 1991; Ermler et al., 1994). The primary donor P is formed by two excitonically interacting bacteriochlorophyll (BChl) *a* molecules (P_L and P_M) that overlap at the ring I position and are related to each other by a C_2 symmetry axis. The energy conversion process in the reaction center is extremely efficient, as it has a quantum yield of near unity. Critical for the achievement of the high efficiency is the electronic structure of P. Ideally, the electronic wavefunctions of P could be calculated from the three-dimensional structure; however, it has proven to be difficult to obtain accurate wavefunctions due to the necessity of incorporating the large macrocycles of P and the many interactions with the surrounding protein (Warshel & Parson, 1987). The availability of site-directed mutagenesis systems for *Rb. sphaeroides* and other purple bacteria [reviewed in

† This work was supported by NSF (MCB9404925) to J.P.A. and by DFG (Sfb 312, TP A4), TU Berlin (FIP 6/12), and Fonds der Chemischen Industrie and Schering AG (Berlin) to W.L.

* Corresponding author.

⊗ Abstract published in *Advance ACS Abstracts,* May 1, 1996.

[1] Abbreviations: BChl, bacteriochlorophyll; BPhe, bacteriopheophytin; P, primary donor; P*, singlet excited state; P^*_{CT}, charge transfer excited configuration; P^*_{EX}, lowest exciton excited configuration; Tris, tris(hydroxymethyl)aminomethane; EDTA, ethylenediaminetetraacetic acid; FT, Fourier transform.

S0006-2960(95)02831-5 CCC: $12.00

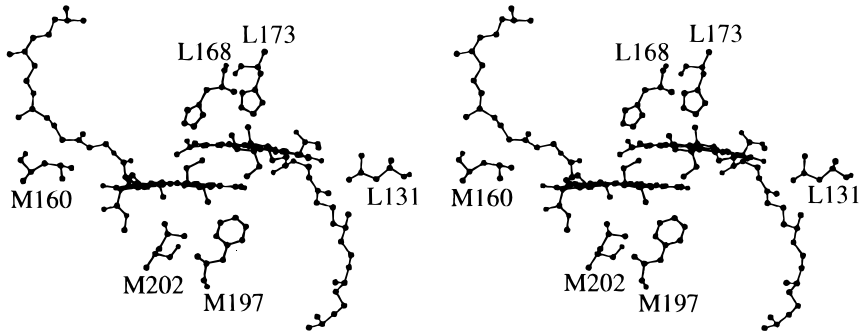

FIGURE 1: Stereoview of the three-dimensional structure of the HL(M202) mutant showing the BChl−BPhe dimer and residues Leu L131, His L168, His L173, Leu M160, Phe M197, and Leu M202. The view is approximately down the 2-fold symmetry axis of the reaction center. The structure determination was reported by Chirino et al. (1994) and coordinates are from the Brookhaven National Laboratory Data Bank, File 1PST.

Williams and Taguchi (1995)] provides the opportunity to make alterations of the amino acids near P and hence change interactions that influence its electronic structure.

Recently, a set of mutants has been designed that alters the number of hydrogen bonds between the protein subunits and the conjugated system of P in *Rb. sphaeroides* [reviewed in Allen and Williams (1995)]. The addition or loss of four histidine residues results in the addition or loss of a hydrogen bond as shown by changes in the vibrational spectra of P (Nabedryk et al., 1993; Mattioli et al., 1994, 1995). The addition of each hydrogen bond between a histidine residue and P was shown to result in a 60−120-mV increase in the P/P^+ midpoint potential without a significant alteration of the energy of the singlet excited state P* relative to the ground state (Stocker et al., 1992; Williams et al., 1992; Murchison et al., 1993; Lin et al., 1994). These changes in the midpoint potential of P are correlated with changes in several of the electron transfer rates of the reaction center [reviewed in Allen and Williams (1995)]. Electron nuclear double resonance (ENDOR) spectroscopy revealed well-defined changes of the electronic structure of P that were modeled assuming that the hydrogen bonds preferentially stabilize one BChl of P relative to the other BChl (Rautter et al., 1995).

Another approach toward modifying the electronic properties of P is to alter the pigments forming P. When one of the axial histidine ligands of P is changed to leucine, the BChl that was coordinated to the histidine is replaced by a bacteriopheophytin (BPhe), resulting in a BChl−BPhe "heterodimer" (Bylina & Youvan, 1988; McDowell et al., 1991). The BPhe is located close to where a BChl is in the wild-type structure, and overall the three-dimensional structure of the heterodimer from *Rb. sphaeroides* is largely unchanged relative to wild type (Figure 1), with His L168 being the only residue forming a hydrogen bond to P (Chirino et al., 1994). Dramatic changes are observed in the properties of the heterodimer, including a 160−180-mV increase in the P/P^+ midpoint potential compared to wild type (Davis et al., 1992; Laporte et al., 1993) and localization of essentially all of the unpaired electron spin density on the BChl molecule of P in its oxidized state (Bylina et al., 1990; Huber et al., 1996). These altered properties are thought to largely arise from the change in composition of P, as a BPhe molecule in solution is 200−300 mV more difficult to oxidize and is a much better electron acceptor than BChl (Fajer et al., 1975; Watanabe & Kobayashi, 1991). The properties of the excited state P* in the heterodimer are also changed, as the optical band associated with the Q_y transition is significantly broader than wild type, and the yield of electron transfer from the excited state is diminished by ∼50% (Bylina & Youvan, 1988; McDowell et al., 1991).

In this work we describe four mutants that have been designed to alter hydrogen bonds between histidine residues and P in the heterodimer. The single heterodimer mutant HL(M202), in which the axial ligand His M202 was changed to Leu, was compared with four double mutants that combine the heterodimer mutation with each one of the hydrogen-bond mutations. Two mutants are designed to introduce hydrogen bonds to the BPhe molecule of the heterodimer: HL(M202)+LH(M160) and HL(M202)+FH(M197) should introduce a hydrogen bond between His M160 (Leu in wild type) and the 9-keto group and between His M197 (Leu in wild type) and the 2-acetyl group, respectively. The mutant HL(M202)+LH(L131) is designed to introduce a hydrogen bond between the 9-keto group of the BChl molecule of P and His L131 (Leu in wild type). The mutant HL(M202)+HF(L168) is designed to remove the hydrogen bond between His L168 and the BChl molecule of the heterodimer in HL(M202). Previously, we have described the construction of the mutants and reported that the spin density distribution of P^+, as measured by ENDOR spectroscopy, is localized on the BChl molecule in all of these mutants, as was found for the HL(M202) mutant (Rautter et al., 1995). In this paper we report several other characteristics of the mutant reaction centers, including the optical spectra, P/P^+ midpoint potentials, Fourier transform (FT) resonance Raman spectra, yields of charge separation, and charge recombination rates. On the basis of the effects observed for the alteration of hydrogen bonds to P in wild type, well-defined and significant changes are expected for the energies of the donor, such as the P/P^+ midpoint potential in the heterodimer/hydrogen-bond mutants. A model is then proposed relating changes in the electronic structure of the heterodimer to the addition or loss of hydrogen bonds.

MATERIALS AND METHODS

Strain Construction and Protein Isolation. The mutants were constructed by oligonucleotide-directed mutagenesis and cloning of restriction fragments as described previously (Rautter et al., 1995). The genes were expressed in the *Rb. sphaeroides* deletion strain ΔLM1.1 (Paddock et al., 1989), which is derived from the wild-type 2.4.1 strain. For all

Table 1: Summary of Results for Heterodimer/Hydrogen-Bond Mutants

strain	alteration of P	BChl/BPhe[a] ratio	E_m[b] (mV)	ΔE_m[c] (mV)	τ_{AD}[d] (ms)
wild type		2.05	505 ± 5		100
HL(M202)+HF(L168)	removes H bond from BChl	1.00	555 ± 5	−85 (−95)	65
HL(M202)	BChl/BPhe heterodimer	1.00	640 ± 10		45
HL(M202)+LH(M160)	adds H bond to BPhe	1.10	655 ± 10	15 (60)	40
HL(M202)+FH(M197)	adds H bond to BPhe	1.00	655 ± 10	15 (125)	40
HL(M202)+LH(L131)	adds H bond to BChl	1.05	720 ± 15	80 (80)	15

[a] Determined by extraction of pigments. Estimated error is ±0.1. [b] P/P^+ midpoint potential versus NHE. [c] E_m (heterodimer/hydrogen-bond double mutant) − E_m (heterodimer single mutant). The number in parentheses is the change in midpoint potential previously described for the corresponding single hydrogen-bond mutant with the BChl dimer compared to wild type, from Lin et al. (1994). [d] Characteristic time for charge recombination from the primary quinone. Estimated error is ±10%.

experiments, the wild-type reaction centers were those isolated from the deletion strain complemented with a plasmid bearing the wild-type genes. The reaction centers were isolated using published procedures (Paddock et al., 1989; Williams et al., 1992; Rautter et al., 1995). The ratio of the absorbance at 280 and 800 nm after isolation was between 1.2 and 1.6. Unless noted otherwise, the protein was in 15 mM Tris-HCl, pH 8, 0.025% lauryldimethylamine *N*-oxide, and 1 mM EDTA.

Pigment Extraction. The relative amount of BChl *a* compared with BPhe *a* was determined by extraction of the pigments from purified reaction centers. The total pigment content from reaction centers was extracted into a 2:7 methanol:acetone solution, mixed, and centrifuged in an Eppendorf microcentrifuge at 8000*g* for 2 min. The optical spectrum of the supernatant was measured and the relative amounts of BPhe and BChl were determined using published extinction coefficients for BChl and BPhe at 771 and 747 nm (Straley et al., 1973; van der Rest & Gingras, 1974).

Steady-State and Transient Optical Spectroscopy. Optical absorption spectra of the isolated reaction centers were measured using a Cary 5 spectrophotometer (Varian). For the measurements at 20 K a helium displex refrigerator (APD) was used with the protein in a glycerol solution as described previously (Williams et al., 1992). Measurements of the spectra at 77 K were performed using a nitrogen-cooled cryostat (DN 1704, Oxford). The transient absorption changes at 295 K were measured using a kinetic spectrophotometer of local design (Kleinherenbrink et al., 1994). A Surelight laser (Continuum) was used to excite the sample with a 5-ns pulse at 532 nm. The time course of the absorbance was monitored between 820 and 900 nm with the protein at an optical absorption A_{802}^{1cm} of 0.5, and 0.5 mM terbutryn was added to block electron transfer to the secondary quinone. The yield of the charge separated state $P^+Q_A^-$ was determined by measuring the extent of bleaching at 865 nm in response to 5-ns pulses at 532 nm as the intensity was varied by use of neutral density filters.

Oxidation−Reduction Titrations. The P/P^+ midpoint potentials of isolated reaction centers were determined by three independent redox titration techniques. The redox potential of the solution was altered either chemically or electrochemically and 2−4 measurements were performed on all samples. One set of measurements was performed at 295 K (at Arizona State University) using an electrochemical cell as previously described (Lin et al., 1994). For these measurements, the reaction centers were in 20 mM Tris-HCl, pH 8, 1 mM EDTA, 0.1% Triton X-100, and 60 mM KCl, with 0.25 mM potassium ferrocyanide and 0.4 mM dicyanobis(1,10-phenanthroline)iron (II) dihydrate (Schilt, 1960) added as mediators. Electrochemical measurements were also performed independently at 277 K (at Technische Universität Berlin) using a cell described in Moss et al. (1991). For these measurements, the reaction centers were in 12.5 mM phosphate buffer, pH 7.4, 0.1% octyl glucoside, and 125 mM KCl, with either 0.25 mM potassium ferrocyanide or 0.4 mM dicyanobis(1,10-phenanthroline)iron (II) dihydrate added as a mediator. A third set of chemical titrations were performed with the reaction centers in 100 mM Tris-HCl, pH 8, 0.05% Triton X-100, and 1 mM EDTA and were titrated using ferricyanide and sodium ascorbate as described previously (Williams et al., 1992).

For all of the redox titrations, the extent of reduction of P was determined by monitoring the absorbance of the dimer Q_y absorption band at different ambient redox potentials. The band changed uniformly as the potential was altered, and for the analysis presented below the absorption at 865 nm was used. The relative amount of reduced P as a function of the ambient potential was fit using the measured absorption, *A*, according to the Nernst equation:

$$(A - A_{ox})/(A_{red} - A) = \exp[(E_m - E)/(RT/nF)] \quad (1)$$

where A_{ox} is the absorbance of the fully oxidized state, A_{red} is the absorbance of the fully reduced state, E_m is the midpoint potential, *E* is the measured ambient potential, *n* is the number of electrons, *T* is the temperature, *R* is the gas constant, and *F* is the Faraday constant. For the chemical titrations, the spectrum of the fully oxidized state, A_{ox}, was measured by light bleaching of the samples and the data were fit using the Nernst equation ($n = 1$) with only one parameter, E_m, allowed to vary. For the electrochemical titrations, two additional parameters, A_{red} and A_{ox}, were also adjusted to produce the best fit while *n* was either fixed equal to 1 or allowed to vary.

Fourier Transform Raman Spectroscopy. The FT Raman spectra of isolated reaction centers were recorded using a Bruker IFS 66 interferometer coupled to a Bruker FRA 106 Raman module as described in detail elsewhere (Mattioli et al., 1991). The spectra were recorded at 15 K and the spectral resolution of 8000 coadded interferograms was 4 cm^{-1}.

RESULTS

Pigment Extraction. For all mutants and wild type the cofactor composition was measured by performing a pigment extraction of isolated reaction centers. For each strain, at least 10 independent extractions were performed. For all reaction centers containing the HL(M202) mutation the

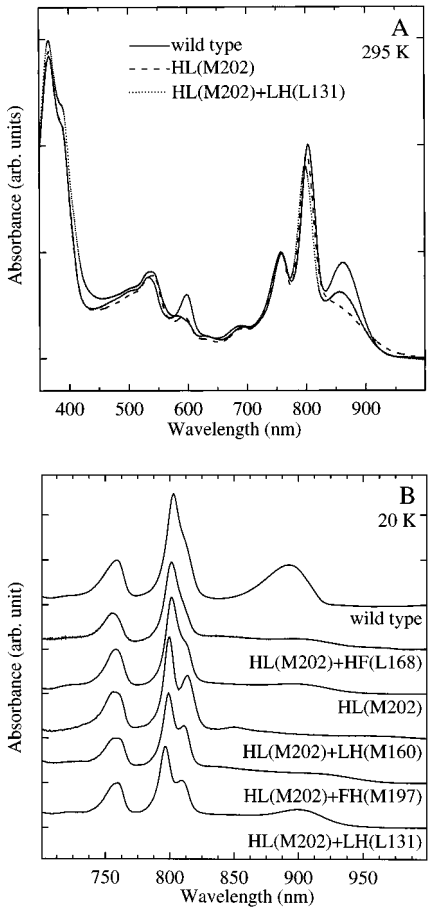

FIGURE 2: Optical absorption spectra of reaction centers from wild type and heterodimer/hydrogen-bond mutants at (A) room temperature (295 K) and (B) low temperature (20 K). Variations among the strains can be seen in the dimer Q_y absorption band, which in wild-type reaction centers is centered at 865 and 890 nm at 295 and 20 K, respectively. Additional resolved transitions in the 800-nm region are observed in the heterodimer/hydrogen-bond mutants compared to the wild type and the HL(M202) single mutant. The spectra have been normalized at 760 nm.

measured BChl/BPhe ratio was ~1.0, and for wild type the ratio was ~2.0 (Table 1).

Optical Absorption Spectra. In contrast to the well-defined Q_y absorption band centered at 865 nm observed for wild-type reaction centers at 295 K, the band for the HL(M202) mutant was very broad with no distinct peak maximum evident (Figure 2A), as has been previously published (Bylina & Youvan, 1988; McDowell et al., 1991). Changes are also present in the absorption bands at 540 and 600 nm due to the altered cofactor composition, as has been discussed previously (Bylina & Youvan, 1988; McDowell et al., 1991).

A significant difference is evident in the 295 K spectrum of HL(M202)+LH(L131) compared with HL(M202) (Figure 2A). The Q_y transition of HL(M202)+LH(L131) has a peak centered at 850 nm that has an appearance more similar to that of wild type than HL(M202). In contrast, the spectra of the other mutants are similar to HL(M202) (data not shown). The 500−600-nm region of the HL(M202)+LH-(L131) mutant is very similar to that of the other heterodimer mutants, indicating that all mutants have the same pigment composition. The corresponding single hydrogen-bond mutant LH(L131) has only small differences in the optical spectrum compared to wild type.

At 20 K, distinct spectral features are observed for all of the mutants in the near infrared region (Figure 2B). For wild type the dimer absorption band is red-shifted to 890 nm and a shoulder is observed at 810 nm. For HL(M202), the dimer Q_y absorption band is broad, extending from approximately 800 to 950 nm, with a slight peak near 900 nm, and the shoulder near 810 nm is somewhat more resolved than in wild type as previously reported (Hammes et al., 1990). For HL(M202)+LH(L131), a resolved peak centered near 900 nm with an underlying broad band from 800 to 950 nm is evident. A much smaller resolved peak near 900 nm is also present in the spectrum of HL(M202)+HF(L168). For the HL(M202)+LH(M160) and HL(M202)+FH(M197) mutants, the Q_y absorption band is very flat and featureless. Resolution of a transition near 810 nm is altered in the double mutants compared to HL(M202). The HL(M202)+LH-(M160) has the clearest resolution with peak maxima at 800 and 815 nm, while the transitions are the least pronounced for HL(M202)+HF(L168). The wavelength of the peak near 800 nm varies for the mutants, with HL(M202)+LH(L131) having a peak maximum at the most blue-shifted wavelength of 796 nm compared to 803 nm for wild type. Similar changes in the resolution of the transitions in the 800-nm region were observed for the corresponding single hydrogen-bond mutants with the BChl dimer (Williams et al., 1992; Murchison et al., 1993; Mattioli et al., 1995). In general, for both the BChl dimer and the heterodimer, the loss of the hydrogen bond at L168 leads to a loss of resolution of the transitions near 800 nm, and the addition of a hydrogen bond to the dimer leads to an enhanced resolution. Molecular orbital models of reaction centers show that this region of the optical spectrum is complex with contributions from several transitions (Parson & Warshel, 1987; Lathrop & Friesner, 1994). Thus, interpretation of the optical spectrum in this region is difficult. However, the observation of similar effects for the two dimer systems suggests that these optical changes reflect specific interactions with the introduced histidine residues. The BPhe absorption band at 760 nm is essentially the same in all of the heterodimer mutants. Likewise, in the 350−700-nm region, the spectra of the double mutants are similar to that of HL(M202) (data not shown). Spectra were also measured at 77 K and found to have similar but somewhat less resolved features compared to 20 K, as previously noted (Hammes et al., 1990).

Charge Recombination and Yield Measurements. The charge recombination times from the primary quinone were measured to be 100 and 45 ms for wild type and HL(M202) respectively, as has been previously reported (Laporte et al., 1993). For the two mutants HL(M202)+LH(M160) and HL-(M202)+FH(M197), times of approximately 40 ms were measured. Significantly different times of 65 and 15 ms were obtained for HL(M202)+HF(L168) and HL(M202)+LH-(L131), respectively. The yield of charge separation has been reported to decrease from 1.0 for wild type to 0.4 for the HL(M202) heterodimer mutant (Kirmaier et al., 1988; McDowell et al., 1991). The yield as measured by the extent of the light-induced bleaching was observed to be significantly diminished to 0.1 ± 0.1 for the two mutants HL-(M202)+LH(M160) and HL(M202)+FH(M197). In contrast, an increase of yield to 0.75 ± 0.15 was determined for HL(M202)+HF (L168), while for HL(M202)+LH(L131) the measured yield of 0.4 ± 0.15 is not changed, within error, compared to HL(M202).

P/P^+ Midpoint Potential. The midpoint potentials were determined at Arizona State University for each of the strains

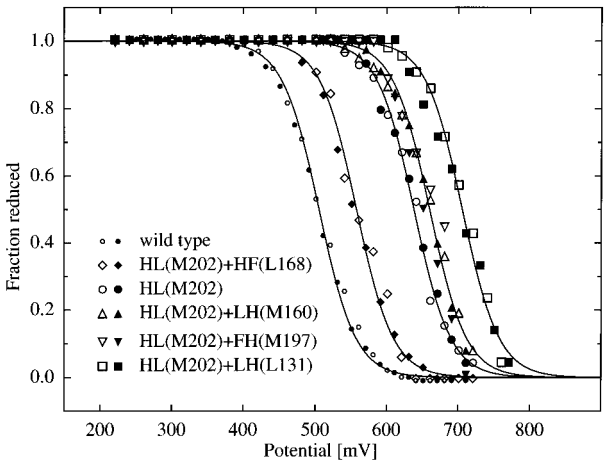

FIGURE 3: Electrochemical oxidation/reduction titrations of P in reaction centers isolated from wild type and the mutants. Oxidative and reduction titrations are indicated by open and closed symbols, respectively. The lines represent fits of the data to the Nernst equation (eq 1) with a single fit shown for the titrations of the HL-(M202)+LH(M160) and HL(M202)+FH(M197) mutants, which have the same midpoint potential. All of the strains containing the heterodimer mutation have higher midpoint potentials than wild type, and the addition of each hydrogen-bond mutation to the heterodimer results in a systematic alteration of the midpoint potential. The values of the P/P^+ midpoint potential based upon several measurements are summarized in Table 1.

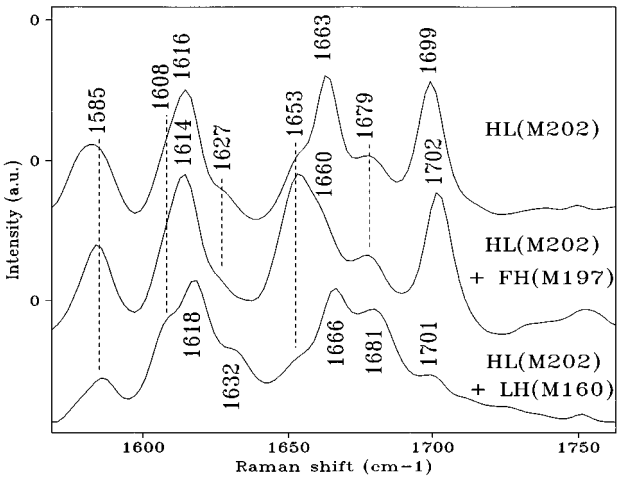

FIGURE 4: Fourier transform preresonance Raman spectra of reaction centers from the HL(M202) heterodimer mutant and the HL(M202)+LH(M160) and HL(M202)+FH(M197) double mutants, which are designed to add a hydrogen bond to the 2-acetyl and 9-keto carbonyl groups, respectively, of the BPhe molecule of P.

from combined oxidative and reductive titrations using the one-electron Nernst equation (Figure 3). The midpoint potentials were also determined independently at Technische Universität Berlin and agreed within the error. The presented values are averages of both measurements (Table 1). For wild type and the HL(M202)+HF(L168) mutant it was possible to fully titrate the samples and the electrochemical data yielded E_m values of 505 and 555 mV, respectively. For these two strains it was also possible to oxidize P chemically using ferricyanide, and fits of those data yielded E_m values of 495 and 540 mV for wild type and HL-(M202)+HF(L168), respectively. For the other mutants E_m values were determined from only electrochemical titrations due to the high P/P^+ midpoint potentials (Table 1). The titrations were nearly complete but the inability to fully titrate the samples resulted in an increase in the error. For HL-(M202) a value of 640 ± 10 mV was obtained. Within the estimated error of ±10 mV, the two mutants HL(M202)+LH-(M160) and HL(M202)+FH(M197) have the same midpoint value of 655 mV. For the HL(M202)+LH(L131) mutant the titration was less complete and consequently the midpoint value of 720 mV has a higher estimated error of ±15 mV.

The value of ~500 mV for wild-type reaction centers is in good agreement with several other previous measurements (Maroti & Wraight, 1988; Moss et al., 1991; Davis et al., 1992; Williams et al., 1992; Nagarajan et al., 1993; Lin et al., 1994). The lower values for the chemical titrations are consistent with previous measurements as noted elsewhere (Lin et al., 1994). A measurement of 658 mV for the His to Leu at M202 heterodimer has been previously reported (Davis et al., 1992). Within the estimated error of 10 mV for each measurement, this agrees with our E_m value of 640 mV for HL(M202).

FT Resonance Raman Spectra. For wild-type reaction centers, excitation at 1064 nm provides preresonance Raman enhancement of both BChls of P. However, for reaction centers containing heterodimers this excitation enhances mainly the BPhe macrocycle of the heterodimer and results in a spectrum that is dominated by the BPhe of P as will be described elsewhere (Mattioli et al., unpublished results). Thus for the mutant strains, spectral changes were only clearly interpretable for the mutants that involved alteration of residues on the M subunit. The spectrum of HL(M202) (Figure 4) has intense bands at 1616, 1663, and 1699 cm^{-1} that have been assigned to the methine bridge, the free 2-acetyl carbonyl, and the free 9-keto carbonyl, respectively, of the BPhe of P (Mattioli et al., unpublished results). For the HL(M202)+LH(M160) mutant, the 1699-cm^{-1} band is downshifted to 1681 cm^{-1}, consistent with the formation of a hydrogen bond between His M160 and the 9-keto group of the BPhe of P. The small band at 1701 cm^{-1} remaining in the spectrum is probably not due to P. For the HL-(M202)+FH(M197) mutant, the 1663-cm^{-1} band is downshifted to 1653 cm^{-1}, showing that His M197 has formed a hydrogen bond to the 2-acetyl group of the BPhe of P. In both cases, the other bands remain essentially unchanged.

DISCUSSION

The heterodimer reaction centers have several distinctive characteristics compared to wild type. The loss of the histidine ligand at M202 results in the incorporation of a BPhe in place of BChl as shown by a variety of spectroscopic measurements (Bylina & Youvan, 1988; Laporte et al., 1993). The BChl−BPhe dimer is also present in the heterodimer/hydrogen-bond mutants as measured by pigment extraction and FT Raman spectroscopy. Preliminary FT infrared spectra of chromatophores show changes compared to wild type, including loss of a band at 2600 cm^{-1}, that confirm the altered composition in the heterodimer/hydrogen-bond mutants (Nabedryk et al., 1995). Compared to wild type, the heterodimer has an increased P/P^+ midpoint potential, loss of yield of electron transfer, and altered optical spectrum (Bylina & Youvan, 1988; Laporte et al., 1993). These characteristics of the heterodimer were modified by the addition or loss of hydrogen bonds as discussed below.

Hydrogen Bonds to P in the Mutants. In wild-type reaction centers, P has only one hydrogen bond to the protein, between the 2-acetyl group of P_L and His L168. The FT

Raman spectra (Figure 4) clearly demonstrate that the presence of His results in the formation of a new hydrogen bond to the 9-keto and 2-acetyl groups of P_M in the HL(M202)+LH(M160) and HL(M202)+FH(M197) mutants, respectively. Due to the weak enhancement of the BChl of P in the heterodimer, the FT Raman data do not provide any conclusive evidence for hydrogen bonds involving P_L. ENDOR measurements indicate that in HL(M202)+LH(L131) a hydrogen bond is formed between His L131 and the 9-keto group of P_L and that the hydrogen bond between His L168 and 2-acetyl group of P_L is broken in HL(M202)+HF(L168) (Rautter et al., 1995).

Relationship between Hydrogen Bonds and P/P$^+$ Midpoint Potential. For the heterodimer, the addition of a hydrogen bond to the BPhe molecule of P results in only a 15-mV increase in the potential compared to increases of 60 and 125 mV observed for the corresponding changes to the BChl dimer in wild type (Table 1). In the heterodimer, the BPhe molecule of P has essentially no unpaired electron spin density in the P^+ state, and correspondingly, there is no charge density on the BPhe (Bylina et al., 1990; Rautter et al., 1995; Huber et al., 1995). The lack of a significant change in the P/P$^+$ potential in the heterodimer as hydrogen bonds are added to the BPhe constituent is consistent with the observation that the removal of the electron upon oxidation is essentially occurring on the BChl molecule. In contrast, the addition of the hydrogen bond to the BChl molecule of the heterodimer resulted in an 80-mV increase in the P/P$^+$ potential, and the loss of the hydrogen bond lowered the potential by 85 mV. For wild type, the midpoint potential changes by +80 and −95 mV for the addition and loss, respectively, of the corresponding hydrogen bonds to the BChl dimer (Table 1). Thus, the alteration of the midpoint potential due to the addition of a hydrogen bond to a BChl is not strongly influenced by the composition of P. A quantitative comparison of the midpoint potential values for the different strains requires determination of possible differences in the strength of the hydrogen bonds (Mattioli et al., 1995); these have not been determined for all of the heterodimer/hydrogen-bond mutants.

Relationship between P/P$^+$ Midpoint Potential and Charge Recombination Rate. A correlation is observed between the rate of charge recombination and the P/P$^+$ midpoint potential for the various mutants. As the P/P$^+$ midpoint potential increases from 555 to 720 mV, the electron transfer time decreases from 65 to 15 ms. The change in P/P$^+$ midpoint potential results in a change in the free energy difference between the final and initial states that determines the rate of electron transfer (Figure 5), as has been demonstrated for the corresponding changes for the BChl dimer in wild type (Lin et al., 1994). However, for a comparable midpoint potential, the charge recombination rate is faster in heterodimer mutants than in the BChl dimer hydrogen-bond mutants. For example, the triple mutant LH(L131)+LH(M160)+FH(M197) has a midpoint potential of 765 mV and a charge recombination time of 40 ms. Therefore the rates cannot be incorporated into the model based on the wild-type BChl dimer, and the limited amount of data for the heterodimer mutants prevents the determination of a unique fit for the dependence of the rate on the free energy difference. An additional complication in modeling the heterodimer data is illustrated by the difference in the rates for the two heterodimers formed by removing the histidine ligand from each side of the dimer reported by Laporte et al. (1993). These mutants have similar midpoint potentials, but the rate of charge recombination is 50 and 100 ms for the M202 and L173 heterodimers, respectively. This discrepancy implies that the heterodimer mutation can cause an additional change that influences the rate.

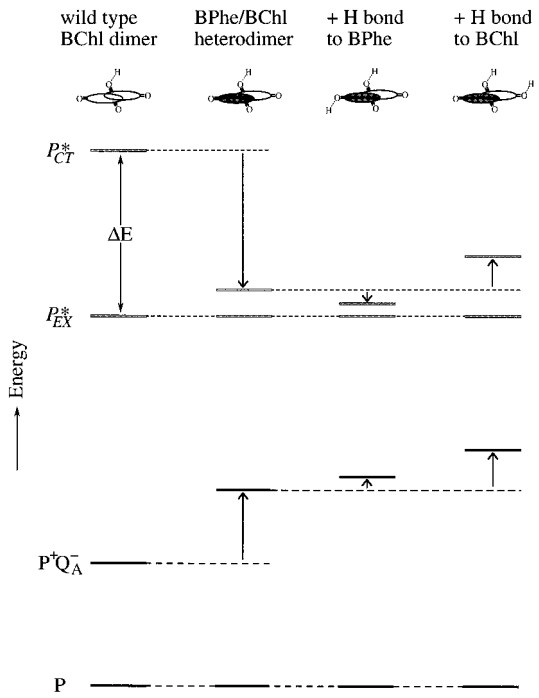

FIGURE 5: Model showing the relative effects of the heterodimer and hydrogen-bond mutations on the energy levels of two electronic states of the reaction center, the ground state (P) and a charge-separated state ($P^+Q_A^-$), and two configurations, the lowest exciton excited state (P^*_{EX}) and the charge transfer excited state (P^*_{CT}). For the purposes of illustration these two configurations are shown as distinct entities, although the basis state P* is a linear combination of these states. The levels of P and P^*_{EX} are assumed to be the same in wild type and the mutants. The increases in the levels of the charge-separated state in the heterodimer single and double mutants correspond to the observed increases in the P/P$^+$ midpoint potentials. In this model, the energy of P^*_{CT} of the HL(M202) heterodimer mutant is decreased relative to wild type. The addition of a hydrogen bond to the BPhe molecule of P in HL(M202)+LH(M160) or HL(M202)+FH(M197) is predicted to stabilize P^*_{CT} compared to HL(M202), while the addition of a hydrogen bond to the BChl molecule of P in HL(M202)+LH(L131) is predicted to destabilize P^*_{CT} relative to that of HL(M202). These changes of P^*_{CT} result in a corresponding alteration of the energy difference ΔE between the P^*_{EX} and P^*_{CT} configurations.

Model for the Effect of Hydrogen Bonds on the Electronic Structure of the Heterodimer. Many of the altered properties of the heterodimer compared to wild type are thought to be due to a change in the nature of P*, in particular the relative contribution of the lowest exciton (P^*_{EX}) configuration and a "charge transfer" (P^*_{CT}) configuration (Kirmaier et al., 1988; Hammes et al., 1990; DiMagno et al., 1990; McDowell et al., 1991; Laporte et al., 1993; Lathrop & Friesner, 1994). The P^*_{CT} configuration is not energetically favorable in the nearly symmetrical BChl dimer of wild type but is much more stable in the heterodimer as a ($BChl^+BPhe^-$) configuration. Stabilization of P^*_{CT} results in a strong mixing between the P^*_{CT} and P^*_{EX} configurations and causes a broadening of the Q_y band in the heterodimer (Lathrop & Friesner, 1994). The energy of P^*_{CT} is not directly observable, but theoretical models estimate the energy difference between the P^*_{CT} and P^*_{EX} configurations, ΔE, as approxi-

mately 3000 and 500−1000 cm^{-1} in wild type and the heterodimer mutant, respectively (Parson & Warshel, 1987; Lathrop & Friesner, 1994).

Changes in hydrogen bonds are expected to have different effects on ΔE depending on the location of the hydrogen bond (Figure 5). The addition of a hydrogen bond to the BPhe molecule of P should stabilize P^*_{CT} and so decrease ΔE. The addition of a bond to the BChl should have the opposite effect of destabilizing P^*_{CT} and increasing ΔE. Based upon the results observed for the BChl dimer (Mattioli et al., 1995), the presence of additional hydrogen bonds should not significantly change the energy of P^*_{EX}. Since all changes are relative to the ground state, the ground state is assumed for simplicity not to change in any mutant compared to wild type. The degree of mixing between P^*_{CT} and P^*_{EX} can be correlated with the shape of the dimer Q_y bands although a detailed interpretation requires application of molecular orbital theory (Parson & Warshel, 1987; Lathrop & Friesner, 1993).

The yield of electron transfer to $P^+Q_A^-$ is determined by the competition between the intrinsic decay rate and the initial electron transfer rate, assuming that there is no yield loss after charge separation. The intrinsic decay rate represents all possible processes that result in the decay of P* except for charge separation. A significant decrease in the initial electron transfer rate or a significant increase in the intrinsic decay rate should result in a decrease in the yield. For HL(M202), the yield has been measured to decrease from 1.0 to 0.4 compared to wild type (Laporte et al., 1993). The yield decrease is thought to arise predominantly from the increased P^*_{CT} contribution to P* that leads to a significantly increased intrinsic decay rate (Laporte et al., 1993). The intrinsic decay time of 30 ps is comparable to the initial electron transfer time of 45 ps for HL(M202). The increase of the initial electron transfer time from 3 ps for wild type is thought to be largely due to the increase in the P/P^+ midpoint potential (Laporte et al., 1993). In general, for the heterodimer/hydrogen bond mutants a decrease in ΔE due to an increased contribution of P^*_{CT} would be expected to increase the intrinsic decay rate, and an decrease in the P/P^+ midpoint potential would be expected to increase the initial electron transfer rate.

For the mutants that added a hydrogen bond to the BPhe molecule of P, HL(M202)+LH(M160) and HL(M202)+FH(M197), the yield of formation of the $P^+Q_A^-$ charge separated state was found to be significantly decreased. The observed decrease in yield is consistent with the model, since the addition of a hydrogen bond in both mutants should decrease ΔE (Figure 5), resulting in an increase in the mixing between P^*_{CT} and P^*_{EX} and hence an increase in the intrinsic decay rate of P*. The presence of a very broad, featureless Q_y band is consistent with these two states being well-mixed.

The addition of a hydrogen bond to the BChl molecule of P in HL(M202)+LH(L131) results in an increase in absorption at 900 nm compared to that observed for HL(M202) (Figure 2). This change in the optical spectrum is consistent with the predicted increase in ΔE, based upon modeling of the absorption spectra of the heterodimer mutants (Lathrop & Friesner, 1993). In contrast to the mutants that add hydrogen bonds to the BPhe molecule, the yield for HL(M202)+LH(L131) was found to be comparable to that for HL(M202). An increase in ΔE would decrease the mixing of P^*_{CT} and P^*_{EX} and hence decrease the intrinsic decay rate of P*. The comparable yields despite a predicted increase in ΔE indicate that the initial electron transfer rate is slower for HL(M202)+LH(L131) compared to HL(M202).

The properties of the HL(M202)+HF(L168) mutant may be more complex than can be explained with this simple model. The yield increases from ∼0.4 to ∼0.75 for HL(M202)+HF(L168) compared to HL(M202). The loss of a hydrogen bond to the BChl side of the heterodimer in HL(M202)+HF(L168) should result in two changes that have opposite effects on the yield, a decrease in ΔE and a decrease in the P/P^+ midpoint potential. To achieve this yield, the expected increase in the intrinsic decay rate of P* for HL(M202)+HF(L168) must be significantly smaller than the increase in the initial electron transfer rate compared to HL(M202). The measured ∼0.75 yield implies that the initial electron transfer rate is ∼3-fold faster than the intrinsic rate of P* decay for HL(M202)+HF(L168). The presence of a very broad band from 800 to 950 nm in the optical spectrum indicates that the energy of P^*_{CT} is above that of P^*_{EX} (Parson & Warshel, 1973). Unlike the other hydrogen bond mutants involving the BChl dimer, the loss of the existing hydrogen bond in HF(L168) results in the energy of P* being shifted by 100−200 cm^{-1} in HF(L168) compared to wild type (Murchison et al., 1993). Structural changes that apparently arise from the loss of the hydrogen bond, most likely rotation of the now free acetyl group of P_L, give rise to changes in the electronic wavefunctions that are comparable to that expected for the loss of the bond (Rautter et al., 1995). Thus, for this mutant, the energies of P^*_{CT}, P^*_{EX}, and P^+ are probably decreased relative to P, although further experimental data is required to determine the extent of these changes.

The addition of the hydrogen bond to the BChl at P_L appears to make the M-side heterodimer similar to the L-side heterodimer, HL(L173). The optical spectrum of HL(L173) has a peak near 860 nm at room temperature and near 900 nm at 1.5 K that is more pronounced than in HL(M202) (Hammes et al., 1990; McDowell et al., 1991). The difference in the optical spectrum of HL(L173) compared to HL(M202) has been modeled as arising from a 500-cm^{-1} larger ΔE (Lathrop & Friesner, 1994). The excited state of HL(L173) has a longer lifetime by a factor of 2−3 compared to HL(M202) that is consistent with an increase in ΔE, although the yield is comparable to that of HL(M202) due to a 2-fold decrease in the rate of charge separation (McDowell et al., 1991). Thus, the similarity of the optical spectra and yield of HL(M202)+LH(L131) and HL(L173) compared to those of HL(M202) suggests that ΔE also increases by 500 cm^{-1} in HL(M202)+LH(L131) due to the addition of the hydrogen bond.

Conclusions. The addition or loss of a hydrogen bond to the heterodimer has a pronounced impact on the electronic structure of P. Significant differences are observed for the addition of a hydrogen bond to the BPhe molecule of P compared to the BChl molecule. The observed changes in the P/P^+ midpoint potentials can be readily explained by comparison with the results of adding a hydrogen bond to the BChl dimer in wild type. The spectral features and observed yields can be qualitatively explained within the framework of a model originally developed for the two heterodimers. This model makes specific predictions concerning the other experimental observables, such as spectral features of the Stark effect and the electron transfer rates.

Once these additional experimental data are available, it should be possible to quantitatively estimate the energy of the internal charge transfer excited state. Hence, studies of these mutants should provide experimental evidence for the energy of the excited state of P that is thought to play a key role in determining the electron transfer properties of the reaction center.

ACKNOWLEDGMENT

We thank X. Nguyen (Arizona State University) and C. Schulz (Technische Universität Berlin) for assistance with the preparation of the reaction centers and U. Fink (Technische Universität Berlin) for help with mutagenesis. We gratefully acknowledge V. Nagarajan and W. Parson (University of Washington) for helpful advice concerning the construction of the electrochemical cell at Arizona State University and E. Hamacher and W. Mäntele (University of Erlanger) for the construction of the electrochemical cell at the Technische Universität Berlin.

REFERENCES

Allen, J. P., & Williams, J. C. (1995) *J. Bioenerg. Biomemb. 27*, 275−283.

Allen, J. P., Feher, G., Yeates, T. O., Komiya, H., & Rees, D. C. (1987) *Proc. Natl. Acad. Sci. U.S.A. 84*, 5730−5734.

Bylina, E. J., & Youvan, D. C. (1988) *Proc. Natl. Acad. Sci. U.S.A. 85*, 7226−7230.

Bylina, E. J., Kolaczkowski, S. V., Norris, J. R., & Youvan, D. C. (1990) *Biochemistry 29*, 6203−6210.

Chirino, A. J., Lous, E. J., Huber, M., Allen, J. P., Schenck, C. C., Paddock, M. L., Feher, G., & Rees, D. C. (1994) *Biochemistry 33*, 4584−4593.

Davis, D., Dong, A., Caughey, W. S., & Schenck, C. C. (1992) *Biophys. J. 61*, A153 (abstr).

DiMagno, T. J., Bylina, E. J., Angerhofer, A., Youvan, D. C., & Norris, J. R. (1990) *Biochemistry 29*, 899−907.

El-Kabbani, O., Chang, C. H., Tiede, D., Norris, J., & Schiffer, M. (1991) *Biochemistry 30*, 5361−5369.

Ermler, U., Fritzsch, G., Buchanan, S. K., & Michel, H. (1994) *Structure 2*, 925−936.

Fajer, J., Brune, D. C., Davis, M. S., Forman, A., & Spaulding, L. D. (1975) *Proc. Natl. Acad. Sci. U.S.A. 72*, 4956−4960.

Hammes, S. L., Mazzola, L., Boxer, S. G., Gaul, D. F., & Schenck, C. C. (1990) *Proc. Natl. Acad. Sci. U.S.A. 87*, 5682−5686.

Huber, M., Isaacson, R. A., Abresch, E. C., Gaul, D., Schenck, C. C., & Feher, G. (1996) *Biochim. Biophys. Acta 1273*, 108−128.

Kirmaier, C., & Holten, D. (1993) in *The Photosynthetic Reaction Center* (Deisenhofer, J., & Norris, J. R., Eds.) Vol. II, pp 49−70, Academic, San Diego, CA.

Kirmaier, C., Holten, D., Bylina, E. J., & Youvan, D. C. (1988) *Proc. Natl. Acad. Sci. U.S.A. 85*, 7562−7566.

Kleinherenbrink, F. A. M., Chiou, H. C., LoBrutto, R., & Blankenship, R. E. (1994) *Photosynth. Res. 41*, 115−123.

Laporte, L., McDowell, L. M., Kirmaier, C., Schenck, C. C., & Holten, D. (1993) *Chem. Phys. 176*, 615−629.

Lathrop, E. J. P., & Friesner, R. A. (1994) *J. Phys. Chem. 98*, 3056−3066.

Lin, X., Murchison, H. A., Nagarajan, V., Parson, W. W., Allen, J. P., & Williams, J. C. (1994) *Proc. Natl. Acad. Sci. U.S.A. 91*, 10265−10269.

Maroti, P., & Wraight, C. A. (1988) *Biochim. Biophys. Acta 934*, 329−347.

Mattioli, T. A., Hoffmann, A., Robert, B., Schrader, B., & Lutz, M. (1991) *Biochemistry 30*, 4648−4654.

Mattioli, T. A., Williams, J. C., Allen, J. P., & Robert, B. (1994) *Biochemistry 33*, 1636−1643.

Mattioli, T. A., Lin, X., Allen, J. P., & Williams, J. C. (1995) *Biochemistry 34*, 6142−6152.

McDowell, L. M., Gaul, D., Kirmaier, C., Holten, D., & Schenck, C. C. (1991) *Biochemistry 30*, 8315−8322.

Moss, D. A., Leonhard, M., Bauscher, M., & Mäntele, W. (1991) *FEBS Lett. 283*, 33−36.

Murchison, H. A., Alden, R. G., Allen, J. P., Peloquin, J. M., Taguchi, A. K. W., Woodbury, N. W., & Williams, J. C. (1993) *Biochemistry 32*, 3498−3505.

Nabedryk, E., Allen, J. P., Taguchi, A. K. W., Williams, J. C., Woodbury, N. W., & Breton, J. (1993) *Biochemistry 32*, 13879−13885.

Nabedryk, E., Breton, J., Kuhn, M., Fetsch, A., Schulz, C., & Lubitz, W. (1995) *Biophys. J. 68*, A93 (abstr).

Nagarajan, V., Parson, W. W., Davis, D., & Schenck, C. C. (1993) *Biochemistry 32*, 12324−12336.

Paddock, M. L., Rogney, S. H., Feher, G., & Okamura, M. Y. (1989) *Proc. Natl. Acad. Sci. U.S.A. 86*, 6602−6606.

Parson, W. W. (1991) in *Chlorophylls* (Scheer, H., Ed.) pp 1153−1180, CRC Press, Boca Raton, FL.

Parson, W. W., & Warshel, A. (1987) *J. Am. Chem. Soc. 109*, 6152−6163.

Rautter, J., Lendzian, F., Schulz, C., Fetsch, A, Kuhn, M., Lin, X., Williams, J. C., Allen, J. P., & Lubitz, W. (1995) *Biochemistry 34*, 8130−8143.

Schilt, A. A. (1960) *J. Am. Chem. Soc. 82*, 3000−3005.

Stocker, J. W., Taguchi, A. K. W., Murchison, H. A., Woodbury, N. W., & Boxer, S. G. (1992) *Biochemistry 31*, 10356−10362.

Straley, S. C., Parson, W. W., Mauzerall, D. C., & Clayton, R. K. (1973) *Biochim. Biophys. Acta 305*, 597−609.

van der Rest, M., & Gingras, G. (1974) *J. Biol. Chem. 249*, 6446−6453.

Warshel, A., & Parson, W. W. (1987) *J. Am. Chem. Soc. 109*, 6143−6152.

Watanabe, T., & Kobayashi, M. (1991) in *Chlorophylls* (Scheer, H., Ed.) pp 287−315, CRC Press, Boca Raton, FL.

Williams, J. C., & Taguchi, A. K. W. (1995) in *Anoxygenic Photosynthetic Bacteria* (Blankenship, R. E., Madigan, M. T., & Bauer, C. E., Eds.) pp 1029−1065, Kluwer, Dordrecht, The Netherlands.

Williams, J. C., Alden, R. G., Murchison, H. A., Peloquin, J. M., Woodbury, N. W., & Allen, J. P. (1992) *Biochemistry 31*, 11029−11037.

Woodbury, N. W., & Allen, J. P. (1995) in *Anoxygenic Photosynthetic Bacteria* (Blankenship, R. E., Madigan, M. T., & Bauer, C. E., Eds.) pp 527−557, Kluwer, Dordrecht, The Netherlands.

BI9528311